Interactions between theory and experiment in the investigation of elementary reactions of importance in combustion†

Michael J. Pilling

Received 8th February 2008
First published as an Advance Article on the web 27th February 2008
DOI: 10.1039/b715767c

Elementary reactions are a central component of models of combustion processes. Rate constants and channel yields are needed for those models. Both experimental and theoretical methods used to determine such rate data are discussed in this *tutorial review*, which is of interest to reaction kinetics and combustion engineering communities. Applications to combustion present particular problems because the conditions required can be well outside the ranges of temperature and pressure accessible to experiment, and the rate data can show a complex dependence on conditions. Under these conditions, the interplay between theory and experiment becomes important.

1. Introduction

Combustion involves complex chemical mechanisms, which are made up of large numbers of elementary chemical reactions.[1] The features of the macroscopic combustion process—the rate at which heat is released, ignition characteristics, rates of production of pollutants—depend on the rates of and the interactions between the microscopic processes—the elementary reactions. Models of, for example, automobile engines incorporate both fluid dynamics and chemistry, to describe the way in which the heat released from the chemical reactions is converted into motion of the pistons. The chemical rate equations are based on a *chemical mechanism*, which is a list of the reactants and products in the combustion process, together with associated rate coefficients and their dependence on temperature and, if appropriate, pressure. The process of constructing chemical mechanisms involves the assembly of an explicit set of reactions, which includes all of the reactions thought necessary. This process starts with an initiation reaction that generates radicals and then examines the reaction of the fuel molecules with radicals, especially H, O and OH. In the process of the degradation of the fuel, larger radicals are also produced and their reactions are central to the overall process. The components of the chemical mechanisms have been elucidated over many decades, and there is a general understanding of the types of reaction to include, although surprises continue to occur.[2] Determining the kinetics of the elementary reactions, the rate coefficients and the reaction products, presents both an experimental and a theoretical challenge. These properties are required under the combustion conditions, which may involve temperatures of thousands of degrees Kelvin and pressures of many bar; direct measurement in the laboratory is difficult under such conditions and some form of extrapolation is needed, often involving theory. Some 'elementary' reactions are quite 'complex'. The reaction between an alkyl radical, such as 1-butyl, with O_2, which is central to many combustion processes, occurs *via* several short-lived intermediates to form several different sets of products whose relative yields depend sensitively on the temperature and pressure.[3] Although the general way in which these reactions occur has been understood for many years, a detailed and quantitative understanding only started to emerge a decade or so ago and is still in progress.

Recent years have seen considerable advances, both experimental and theoretical, in the study of elementary reactions of relevance to combustion. Perhaps most interesting has been the increasing convergence of and interaction between experiment and theory. This review examines these two areas of activity.

Section 2 briefly reviews the main experimental methods used to study elementary reactions. The methods used to study macroscopic systems—flames and combustors generally—which have been used to evaluate chemical mechanisms and models and identify sensitive reactions requiring further study are briefly addressed. Section 3 gives a very brief account of the application of electronic structure theory to the calculation of potential energy surfaces for elementary reactions. For simple, single step reactions, such as H abstraction, theory involves the calculation of the rate coefficient using transition

School of Chemistry, University of Leeds, Leeds, UK LS2 9JT
† One of a collection of reviews on the theme of gas kinetics.

Mike Pilling moved in 1989 from Oxford to Leeds as Professor of Physical Chemistry. His research on reaction kinetics spans experimental and theoretical studies on elementary reactions and chemical mechanisms for atmospheric chemistry and combustion. He recently retired as Director of Composition Research at the National Centre for Atmospheric Science and is the Chair of the Air Quality Expert Group.

 This journal is © The Royal Society of Chemistry 2008

state theory. Reactions involving intermediates, sometimes several intermediates, require a more detailed approach. The master equation, ME, approach is described in section 4. This method is the one most generally used and it expresses clearly the timescales of the component reactions, as well as providing a practical approach to modelling reactions and interpreting and extrapolating experimental results. Section 5 provides some case studies of elementary reactions, based on both experimental and theoretical analyses.

2. Experimental methods

Two methods are widely employed in the study of elementary combustion reactions, laser flash potolysis (LFP) and shock tube (ST) techniques. The former are generally restricted to low temperatures (<1000 K), but have the advantage that multiple shot averaging techniques can be used, giving rise to high sensitivity in terms of the radical concentrations that can be measured. This means that secondary (radical + radical) reactions can be minimised so that the decay of the monitored radical is less affected by secondary reactions. The low temperature restriction, though, means that some form of extrapolation is needed for higher temperature applications. ST is essentially a single pulse method, so signal averaging is not feasible. Careful design has led to remarkable increases in sensitivity in recent years.

In LFP, radiation from a pulsed laser, usually operating in the UV, is used to photodissociate a precursor to form the radical under study.[4] An example is OH that can be formed, for example, from *tert*-butylhydroperoxide.[5] Sometimes a combination of photolysis and reaction is used, for example in the formation of C_2H_5 from Cl + ethane, following pulsed photolysis of Cl_2 to form Cl[6] (see section 5). A wide range of detection techniques can be used with LFP, including laser induced fluorescence (LIF),[5] UV and IR absorption spectroscopy[7] and mass spectroscopy.[8] Absorption spectroscopy has been augmented over the last decade or so by cavity ring down and cavity enhanced spectroscopy in which the absorption signal is considerably enhanced by multiple reflections of selected single frequency laser radiation in an optical cavity.[9] In all cases, the signal/noise ratio is improved by repeating the experiment many times and then averaging the signal. Section 5 discusses applications using LIF and IR absorption spectroscopy.

Shock tubes are used for higher temperatures and require high sensitivity detection methods because they are single shot methods, so that signal averaging cannot be used. A high pressure gas propagates through the reaction mixture and compressively heats it. The radical under study is produced by pyrolysis of a precursor, on a timescale that is short compared with the reaction time. Srinivasan *et al.*[10] used the pyrolysis of methanol to form OH and studied its reaction with C_2H_2 over the temperature range 1509–2362 K by absorption spectroscopy at 308 nm, using an OH resonance lamp—a microwave discharge through water in Ar. Oehlschlaeger *et al.*[11] studied H + benzyl over the temperature range 1256–1667. They produced H from the pyrolysis of ethyl iodide and benzyl from toluene and monitored the benzyl by laser absorption at 266 nm. In both cases, it was necessary to take account of secondary reactions, using a model of the competing reactions. To demonstrate the validity of the methods, sensitivity analysis was used to show that the reactions under study made the major contribution to the radical signal decay.

Observations of a range of macroscopic combustions systems, such as flames, are used to probe conditions (*e.g.* temperature and fluid flow) and concentrations of both closed shell and radical species. The results of such experiments are used to evaluate the components of combustion models, including chemical mechanisms. Sensitivity analysis can be used to probe which elementary reactions play a key role in aspects of the mechanism. The methods used have been recently reviewed by Kohse-Höhinghaus *et al.*[12]

3. Electronic structure calculations

There have been substantial improvements in recent years in *ab initio* calculations of potential energy surfaces for gas phase reactions of radicals and they now form a key element in the determination of rate coefficients for combustion reactions involving relatively small numbers of atoms.[13] It is now feasible to calculate energies of transition states to an accuracy of 2–5 kJ mol^{-1}, and this is comparable with the accuracy of experiments. These energy uncertainties affect the rate coefficient through the exponential term in the Arrhenius expression and, at this magnitude, introduce comparatively little error at temperatures of, say, 1000 K (5 kJ mol^{-1} corresponds to a factor of ~ 2 in the exponential term at 1000 K). For reactions with well-defined barriers, it is sufficient to apply transition state theory with a rigid rotor harmonic oscillator model for the reactants and the transition state. This requires information on the energy of the transition state and the geometries and vibrational frequencies of the reactants and transition state. For H atom transfer reactions, tunnelling may also be important. Some reactions, for example radical combinations, occur without a well-defined transition state. In such cases, the position of the transition state varies with the energy in the reacting system and it is necessary to use a variational model, which requires information on energies, geometries and vibrational frequencies along the reaction coordinate. Harding *et al.*[13] have recently reviewed *ab initio* methods for reactive potential energy surfaces and include a brief review of the methods available, as well as a discussion of results for a range of reactions of importance in combustion.

4. Master equation calculations

Reactions such as the dissociation of ethane to form methyl radicals involve collisional excitation to form an energised species, C_2H_6*, with sufficient energy to dissociate. The dissociation takes place in competition with collisional stabilisation:

$$\begin{array}{c} C_2H_6 + M \rightleftharpoons C_2H_6^* + M \\ \downarrow \\ 2CH_3 \end{array}$$

This simple mechanism forms the basis of the Lindemann–Hinshelwood (LH) model for unimolecular dissociation.[14] It leads to an overall rate coefficient that increases with [M] at low pressures, where collisional excitation is the rate determining step, and reaches an asymptote at high pressure, where collisional excitation and stabilisation are rapid, C_2H_6 and C_2H_6* are in equilibrium, and dissociation is the rate determining step.

The model suffers from two major simplifications. The first arises because the rate coefficient for dissociation depends on the internal energy of ethane—the more energy it contains, the more rapidly it dissociates; the LH model assumes that the rate coefficient for dissociation is independent of energy. The second simplification is the so-called *strong collision* assumption, which states that deactivation is a single step process—*i.e.* an energised ethane molecule is completely stabilised in a single collision. A *weak collision* model, in which energy is removed in small steps in a series of collisions, is more realistic.

A *master equation* (ME) model is used to incorporate these improvements.[15,16] The energy levels in ethane are 'bundled' together in *grains*, each grain having a width, typically, of 0.5 kJ mol^{-1}. A rate equation is then set up for each grain:

$$\frac{dc_i}{dt} = -k_i c_i - [M]\sum_j k_{ji} c_i + [M]\sum_j k_{ij} c_j \qquad (E1)$$

where c_i is the concentration of ethane in the ith grain, k_i is the rate coefficient for dissociation fron grain i, k_{ji} is the rate constant for collisional energy transfer from grain i to grain j and M is the diluent gas. It is generally assumed that the probability, P_{ji}, of collisional transfer from grain i to a lower grain j falls off exponentially with the energy difference, so that

$$P_{ji} \propto \exp\left(\frac{-\Delta E}{\langle \Delta E_{down}\rangle}\right)$$

where $\langle \Delta E_{down}\rangle$ is a parameter usually obtained by fitting to experimental data, and ΔE is the energy separation of the grains. The probability P_{ij} for transfer from grain j to grain i, where grain i lies at higher energy, is obtained from P_{ji} using detailed balance, *via* the Boltzmann distribution; knowledge of the numbers of states in each grain is required for this calculation. Application of detailed balance in this way ensures that, following a perturbation and in the absence of reaction, the distribution of molecules throughout the grains tends to a Boltzmann distribution at long times. k_{ij}[M] and k_{ji}[M] are now replaced by ωP_{ij} and ωP_{ji} where ω is the collision frequency at bath gas concentration [M].

The whole set of coupled differential equations for all the grains can be expressed in matrix form:

$$\frac{d\mathbf{c}}{dt} = 2\mathbf{K}\mathbf{c} \qquad (E2)$$

where **c** is a vector of grain concentrations and **K** is a matrix containing the first order and pseudo first order rate constant terms in eqn (E1). Eqn (E2) is solved by an eigenvalue analysis, which gives the eigenvalues and associated eigenvectors of **K**. The eigenvalues are all real and negative, showing that the system evolves in time as a sum of exponential decays.

The eigenvalues of larger magnitude, corresponding to the faster exponential decays, relate to collisional relaxation. In most circumstances, this relaxation occurs on times which are small compared with the overall reaction time. The eigenvalue of smallest magnitude, λ_1, corresponding to the slowest exponential decay, is equal in magnitude to the unimolecular rate coefficient for dissociation: $\lambda_1 = -k_{uni}$. Thus the unimolecular rate coefficient, the target of the master equation calculation, can be obtained from the eigenvalue analysis.

The ME is readily extended to reactions involving association, isomerisation and dissociation reactions to give one or several sets of products. For example, in the reaction

$$A + B \rightleftharpoons C \rightleftharpoons D \rightarrow E + F$$

the reactants A and B associate to form an energised isomer C, which can be collisionally stabilised or can isomerise to form D, which in turn can isomerise back to C, be collisionally stabilised, or dissociate to form products, E + F. The concentration vector, **c**, now contains the concentrations of all the grains in both the isomers C and D. If the reaction is carried out under pseudo first order conditions, such that [A] $\ll$ [B], then one element in **c** contains the concentration of A and [B] is included in the pseudo first order rate coefficient for association. The matrix **K** contains the collisional energy transfer terms in each isomer well, and microcanonical rate constants for isomerisation between isoenergetic grains in wells C and D. It also contains rate constants for association into specific grains in any well connected to the reactants (C in this case) and of dissociation from wells (D in this case) to sets of products to which they are connected. These processes are illustrated below for the reaction H + SO_2. The product species are termed *sinks* (E + F) and are not themselves included in **c**.

The number of eigenvalues again corresponds to the number of elements in **c**, *i.e.* to the total number of grains. The eigenvalues of largest magnitude relate to collisional relaxation, but there are now several eigenvalues relating to rate coefficients for chemical reactions; these have been termed the *chemically significant eigenvalues (CSE)*.[16] The number of such eigenvalues is equal to the number of chemical species contained in the vector **c**, *i.e.* to the number of isomer wells plus the reactant, A. The number of CSE in the above case is, therefore, 3. Generally speaking these eigenvalues are those of lowest magnitude, although at high temperatures they may become comparable in magnitude to the numerically smallest relaxation eigenvalues. The relationship between the eigen values and the rate constants for individual reaction steps can be quite complex and is discussed further in section 5.

Section 5 gives examples of the application of these methods to increasingly complex reactions. Section 5.1 examines simple association reactions under conditions where there is no reaction from the adduct well other than reverse dissociation to the reactants. Section 5.2 discusses two types of reaction system. The first involves the reaction of an alkyl radical with O_2 and the competition between stabilisation of the adduct, a peroxy radical, and its dissociation to form an alkene + HO_2. Under the experimental conditions studied, this reaction can be treated using a model with a single well and a single sink. The next reaction, H + SO_2, involves two isomer wells and a sink and shows the complicated behaviour of the chemically

 This journal is © The Royal Society of Chemistry 2008

significant eigenvalues and their relationship to the rate coefficients.

5. Examples of applications

5.1 Pressure dependence of association reactions

OH adds to both ethene and ethyne to form an adduct, C_2H_nOH:

$$OH + C_2H_4 + M \rightarrow C_2H_4OH + M \quad (1a)$$

$$OH + C_2H_2 + M \rightarrow C_2H_2OH + M \quad (1b)$$

In the atmosphere, C_2H_nOH reacts with O_2 (see below). At the higher temperatures found in combustion systems, the OH adduct can dissociate to form a range of products. Models for combustion and for atmospheric chemistry require rate coefficients as a function of temperature and pressure, and also the yields of the various product channels, again as a function of T and p.

At low temperatures, where OH adduct formation dominates the mechanism, the rate coefficient shows a pressure dependence like that discussed for C_2H_6 dissociation in section 4. At low pressures, the rate determining step is stabilisation of the nascent energised adduct $C_2H_nOH^*$ and the rate constant increases with [M]. At high pressures, the system reaches an asymptote, where every energised adduct formed is stabilised.

Both reactions have recently been studied experimentally, using laser flash photolysis at temperatures between 200 and 400 K.[5,17] Fig. 1 shows the temperature and pressure dependence of the rate coefficient for reaction (1a). k_{1a} depends on pressure, approaching a limit, $k_{1a,\infty}$ as the pressure increases. The high pressure limit is more closely approached at 1 bar pressure ($\sim 2.4 \times 10^{19}$ molecule cm^{-3} at 298 K) at low T than at high T. This is because the higher thermal energy of the reactants gives the adduct more internal energy at higher temperatures, increasing its rate of dissociation so that higher pressures are required for stabilisation.

Fig. 2 shows a similar plot for reaction 1b. The most obvious qualitative difference between the plots is that $k_{1a,\infty}$, increases with decreasing temperature, while $k_{1b,\infty}$ increases

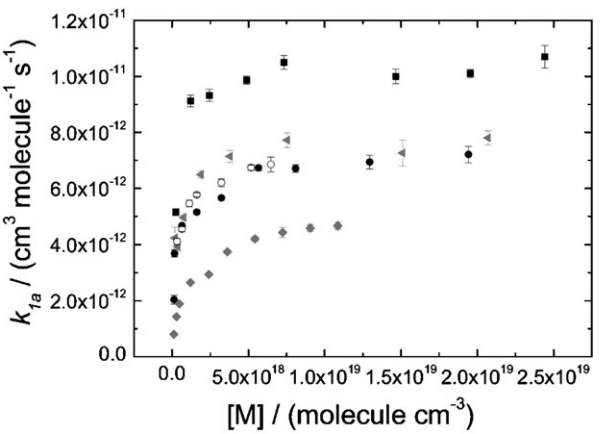

Fig. 1 Bimolecular rate constants for OH + C_2H_4 at 200 K (■) 260 K (grey ◀), 295 K (●) and 400 K (grey ◆) in He and at 295 K in N_2 (○).[5]

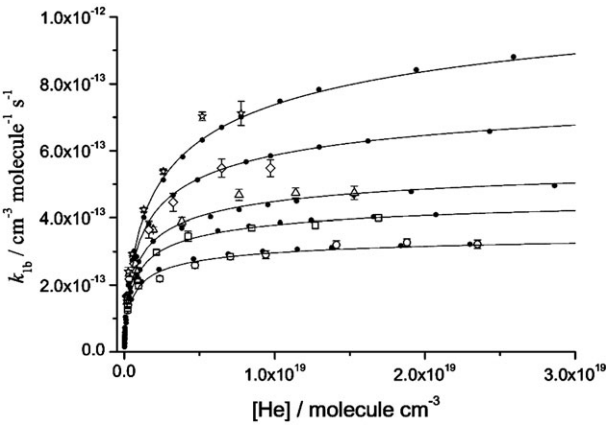

Fig. 2 Bimolecular rate constants for OH + C_2H_2 at 210 (○), 233 (□), 253 (△), 298 (◇) and 373 K (☆) in He. Also included are the master equation fits to this dataset, (●), and a modified Troe fit to the master equation data, solid lines.[17]

with increasing temperature. This is because reaction 1b has a small activation barrier, while reaction 1a has not. The potential energy surfaces for the reactions each have a small attractive potential energy well before the transition state, arising from van der Waals interactions between the reactants. This is then followed, for reaction 1b, by the transition state that lies at an energy greater than that of the reactants; for reaction 1a the transition state energy is less than that of the reactants—a so-called submerged transition state.

The data for reactions 1a and 1b were analysed using a master equation method.[5,17] The high pressure limiting rate coefficients were linked to the microcanonical rate constants for dissociation of the adduct, $k(E)$, using an inverse Laplace transform method[18] that allows $k(E)$ to be related to the Arrhenius parameters, A and E_{act} for the association reaction: $k_\infty = A \exp(-E_{act}/RT)$. The data over the whole range of temperature and pressure were then fitted with these two parameters and the energy transfer parameter, $\langle \Delta E_{down} \rangle$ (see section 4), as variables. The ME calculations were repeated many times, with different parameter values and the best fit values determined as those providing the minimum value of χ^2, the squares of the differences between the calculated and experimental values at a particular T and p, summed over all experimental data points. Fig. 2 shows the master equation fits to the data as filled circles for k_{1b}. These best fit ME data were then used to obtain an analytic form for $k_{1b}(T, p)$, using a standard form used widely in combustion chemistry (a so-called Troe expression[19]); this is shown in Fig. 2 as a set of smooth curves. The same procedure was adopted for $k_{1,a}$.

The following Arrhenius expressions were obtained for the high pressure limiting rate constants:

$$k_{1a,\infty} = 5.0 \times 10^{-12} \exp(148/T) \text{ cm}^3 \text{ molecule}^{-1} \text{ s}^{-1}$$

$$k_{1b,\infty} = 7.3 \times 10^{-12} \exp(-637/T) \text{ cm}^3 \text{ molecule}^{-1} \text{ s}^{-1}$$

Note the opposite signs of the effective activation energies.

Klippenstein and coworkers[20,21] used theoretical methods to obtain a quantitative understanding of this behaviour. Their more detailed analysis was for reaction 1a, where they showed

that the position of the effective transition state for the reaction changes its position with temperature.[21] At very low temperatures, below 130 K, the reaction rate is dominated by an *outer* transition state that lies at larger reactant distances than the van der Waals well, while at higher temperatures, an *inner* transition state, related to the submerged barrier discussed above, dominates. In order to cover the temperature range from 10–600 K, a more complex expression was needed for $k(T)$ than was found experimentally, but the rate coefficient decreased with increasing temperature under all conditions; this behaviour is related to the submerged inner transition state. Similar behaviour was found for reaction 1b,[20] except that the T dependence is positive, because the inner transition state lies above the energy of the reactants.

Senosiain *et al.*[20] also examined the potential energy surface for OH + C_2H_2 to investigate rate processes at higher temperatures. They found that adduct formation becomes unimportant for $T > 1000$ K, except at very high pressures. Formation of H + ketene is the main channel below 2000 K and is superseded by the abstraction reaction forming C_2H + H_2O above ~2000 K. The shock tube measurements of Srinivasan *et al.*,[10] (section 2) investigated the reaction in this temperature regime.

5.2 Reactions involving several wells

5.2.1 Oxidation of hydrocarbons: reactions of peroxy radicals. The oxidation of hydrocarbons below ~1000 K involves a process known as *autoignition* which is related to pressure induced ignition in diesel engines and to 'knock' in petrol (spark ignition) engines.[22] Low temperature alkane oxidation occurs by the mechanism shown schematically in Fig. 3.[3] The parent alkane, RH, reacts with a radical, usually OH, and loses a hydrogen atom to form an alkyl radical R. In general, R undergoes three types of reaction: addition of oxygen to form a peroxy radical (1), decomposition to an alkene, A_1, and a smaller alkyl radical, R_1, (2) or reaction with O_2 to produce the conjugate alkene, A_2 (with the same number of carbon atoms as the parent) and an HO_2 radical (3).

$$R + O_2 \rightleftharpoons RO_2 \quad (1)$$

$$R \rightarrow R_1 + A_1 \quad (2)$$

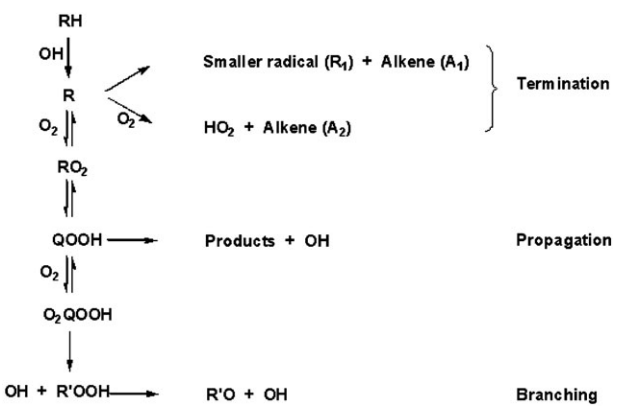

Fig. 3 Simplified outline mechanism for the low temperature oxidation of an alkane, RH. QOOH is an alkyl hydroperoxide radical, formed from RO_2 by internal H atom transfer.

$$R + O_2 \rightarrow A_2 + HO_2 \quad (3)$$

There has been continuing discussion of the mechanism of reaction (3); it is now clear, as discussed below, that it occurs *via* the peroxy radical rather than *via* direct abstraction.

The peroxy radical, RO_2, can also undergo an internal hydrogen abstraction to form a hydroperoxide group (–OOH) and a new alkyl radical centre further along the carbon chain.

$$e.g.\ CH_3CH_2CH_2CH_2O_2 \rightarrow CH_3CHCH_2CH_2OOH$$

The product of this peroxy radical isomerisation is commonly denoted as QOOH:

$$RO_2 \rightarrow QOOH \quad (4)$$

QOOH can cyclise, to form OH and a cyclic ether with ring sizes from 3 to 6 atoms. Other products, such as aldehydes, can also be formed as co-products of OH. The importance of the QOOH route increases as the size of the alkyl group increases; it is relatively unimportant for $C_2H_5O_2$, which is one of the more fully investigated peroxy radicals.

QOOH is an alkyl radical and can add another O_2. Subsequent isomerisation of the peroxy radical so formed produces, through an unstable intermediate, a molecular (non-radical) hydroperoxide, R′OOH, and an OH radical, *e.g.*

$$CH_3CHCH_2CH_2OOH + O_2 \rightarrow CH_3C(O_2)HCH_2CH_2OOH$$

$$CH_3C(O_2)HCH_2CH_2OOH \rightarrow CH_3C(OOH)HCH_2CHO + OH$$

$CH_3C(OOH)HCH_2CHO$ is the hydroperoxide R′OOH. It is not a radical and has a significant lifetime, particularly at the lower end of the temperature range, but the O–OH bond is quite weak. Dissociation leads to the formation of two radicals, one of which is OH.

$$R'OOH \rightarrow R'O + OH \quad (5)$$

This reaction increases the number of radicals in the system, and so is similar to the *branching* steps in the hydrogen + oxygen reaction, that can lead to explosive behaviour, *e.g.*

$$H + O_2 \rightarrow OH + O.$$

However, R′OOH is much less reactive, and is longer-lived than H, so that there can be a significant time delay before dissociation, accompanied by an accelerating reaction rate, occurs. In consequence, R′OOH is termed a *degenerate branching agent*. Its thermal decomposition to two radicals is the branching step in the mechanism: it provides the increase in the number of radicals needed for the runaway phenomenon of autoignition. A hydroperoxide, ROOH can also be formed by H abstraction by RO_2 from RH, and provides another route to branching.

The termination steps which moderate or prevent this runaway are those early in the mechanism producing inert radicals, HO_2 (reaction (3)) and small alkyl radicals (reaction (2)), such as CH_3. The competition in the reactions of R and RO_2, shown in Fig. 3, has the important consequence that branching is greatly favoured, and autoignition enhanced, when peroxy isomerisations are facile, since the route to branching involves two such reactions, while that to termination involves

 This journal is © The Royal Society of Chemistry 2008

none. Isomerisation is easiest in long straight alkane chains and large *n*-alkanes autoignite under milder conditions than small or branched alkanes.

Another significant and related feature of the mechanism is connected with the reversibility of the formation of RO_2 (reaction (1)). As described above, the subsequent chemistry of RO_2 radicals leads to branching while termination occurs through the alkyl radical R. At higher temperatures the equilibrium in reaction (1) shifts to the left and the termination reactions through R are favoured over the branching reactions through RO_2, so that the reaction gets slower. This results in a region of negative temperature coefficient,[23] where the rate decreases as the temperature is raised.

All of these ideas were developed through indirect experiments, especially by Walker and his co-workers.[3] In the last few years there have been several key experiments using laser flash photolysis that, coupled with theory, have considerably enhanced our understanding of reactions of peroxy radicals.

The most detailed experimental studies of ethyl + O_2, and of the product channels, have been made by Taatjes and co-workers.[6,24] They coupled laser flash photolysis to infra-red absorption spectroscopy to detect HO_2 and to LIF to detect OH, producing C_2H_5 from Cl + C_2H_6, following photolysis of Cl_2 or $CFCl_3$ to form Cl. They measured the *absolute* yields of HO_2 in reaction (3), calibrating the HO_2 signal by replacing the C_2H_6 by CH_3OH. The radical products of the Cl + CH_3OH reaction (CH_2OH, 85% yield and CH_3O 15% yield at room temperature) both react with O_2 to give HO_2, which is thus formed in 100% yield in the Cl + CH_3OH + O_2 system. The OH LIF signal was calibrated by converting the HO_2 from Cl + CH_3OH + O_2 to OH by reaction with NO.

Fig. 4 shows HO_2 traces at 423 K and 648 K, respectively. At the lower temperature, HO_2 is formed on a very short timescale from both C_2H_6 and CH_3OH, by the R + O_2 reaction and then decays on a much longer timescale primarily by HO_2 + HO_2. The yield of HO_2 from C_2H_6 is clearly much less than that from CH_3OH, *i.e.* much less than unity. At the higher temperature, HO_2 is again formed on a short timescale from C_2H_5 + O_2, but the signal continues to rise as HO_2 is generated on a longer timescale. The slower rise reflects HO_2 formation from the dissociation of collisionally stabilised $C_2H_5O_2$, with the faster component deriving directly from energised peroxy radical, $C_2H_5O_2$*, formed from the C_2H_5 + O_2 reaction, without any collisional stabilisation taking place. Fig. 5 shows the temperature dependence of the total yield of HO_2, demonstrating its initially slow and then more rapid increase with T; at 700 K, the yield of HO_2 is close to unity. These results are entirely compatible with earlier experimental results, but now provide much more detailed information on the time dependence of HO_2 formation and demonstrate clearly that the mechanism involves the peroxy radical, rather than direct abstraction of H from C_2H_5 by O_2. Similar results are shown for propane. The yield of OH, formed from QOOH, is much smaller, reaching $\sim$1% at the highest temperature studied (700 K).

All of these experiments are compatible with a model for C_2H_5 + O_2 based on reactions (1) and (3), but with reaction (3) occurring *via* an energised peroxy radical rather than a direct abstraction as was at one time proposed. The most

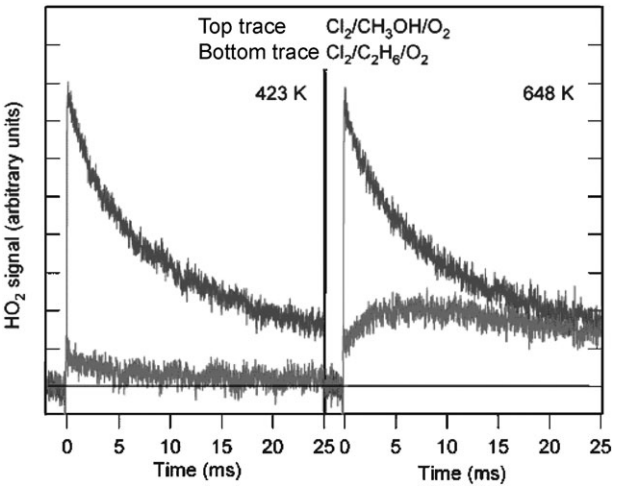

Fig. 4 Measurements of HO_2 formed by the Cl-initiated oxidation of ethane at two temperatures. The top traces are HO_2 formed by the reference reaction system of Cl-initiated methanol oxidation, which transforms the initial Cl atom concentration quantitatively into HO_2. The bottom traces are HO_2 formed from the Cl-initiated oxidation of ethane.[23]

detailed theoretical analysis of the experimental results was undertaken by Miller and co-workers.[25,26] Fig. 6 shows schematically their potential energy surface and demonstrates that there is a low energy route from $C_2H_5O_2$ to HO_2, with the barrier below the energy of the reactants, C_2H_5 + O_2. It is a *concerted* elimination of HO_2 from the peroxy radical, *i.e.* a single step reaction, not involving an intermediate. OH can be formed directly from $C_2H_5O_2$, together with ethanal, *via* a high energy channel, or *via* the hydroperoxide, C_2H_4OOH, with oxirane as the co-product. The higher energies of the transition states for these channels, compared with that for HO_2 formation, provides a rationalisation of the relative yields of OH and HO_2.

Miller and Klippenstein[26] employed a master equation analysis, using data from the potential energy surface calculations, in order to obtain a more quantitative analysis of the

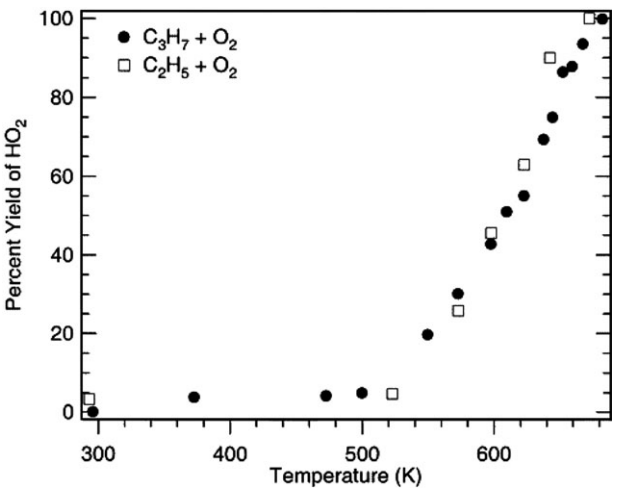

Fig. 5 Comparison of the total yield of HO_2 *vs.* T for propyl and ethyl + O_2 at a constant total density of diluent gas.[6]

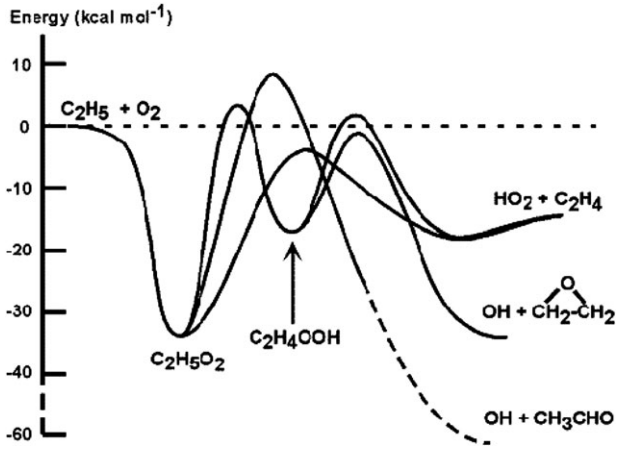

Fig. 6 Potential energy surface for ethyl + O_2. HO_2 is formed in a concerted mechanism from $C_2H_5O_2$, while there are two higher energy routes to OH, one of which involves isomerisation of C_2H_4OOH.[24,25]

experimental results. They examined the two eigenvalues of smallest magnitude, related these to the phenomenological rate constants for the system, and compared their analysis with the experimental data obtained by Taatjes and co-workers.[6,24] They found that they needed to include only the well for $C_2H_5O_2$ in their analysis, since the higher energy barriers preclude significant reaction through the hydroperoxy radical. They showed that the reaction can be characterized by three different regimes:

(i) At low temperatures ($T < 575$ K), the system can be described by reactions (1) and (3). The overall rate coefficient is pressure dependent, and the fractional yield for the channel leading to $C_2H_4 + HO_2$, α, decreases with pressure, in agreement with experiment, because of the collisional stabilisation of $C_2H_5O_2$*. At any given pressure, α increases with temperature because the energised peroxy radical has more energy at higher temperatures and is less easily stabilised. In this temperature regime, the $C_2H_5O_2$ is stable on the experimental timescale of the $C_2H_5 + O_2$ reaction and the eigenvalue related to its dissociation to form $C_2H_4 + HO_2$ is very small in magnitude. Reaction (3) derives entirely from dissociation of $C_2H_5O_2$*, formed from the reactants $C_2H_5 + O_2$. It is termed an *indirect* reaction: the transition state leading to products is not directly connected to the reactants.

(ii) At intermediate temperatures ($575 \leq T/\mathrm{K} \leq 750$) the system becomes more complex, because both the reverse reaction (−1) and dissociation of thermalised $C_2H_5O_2$ to form $C_2H_4 + HO_2$ become significant; the chemical lifetimes of C_2H_5 and $C_2H_5O_2$ are now becoming comparable. From the master equation viewpoint, the two eigenvalues of smallest magnitude, which relate to the overall chemical processes that are significant on the experimental timescale, become comparable in magnitude.

As discussed above Taatjes and co-workers[6,24] studied this regime experimentally, and found two reaction timescales (Fig. 4): prompt, which derives from the formation of HO_2 from $C_2H_5O_2$*, formed directly from $C_2H_5 + O_2$, and slow which relates to formation from dissociation of thermalised $C_2H_5O_2$. This phenomenological description becomes less satisfactory as the temperature increases and the timescales become closer in magnitude. It is then no longer feasible to associate the eigenvalues—which determine the timescales—*directly* with rate coefficients for specific reactions. Miller and Klippenstein[26] have provided a detailed discussion of the kinetic behaviour of the $C_2H_5 + O_2$ reaction, in this temperature regime, within the framework of the master equation.

(iii) At higher temperatures, $T/\mathrm{K} \geq 750$, the system can once again be described by a single eigenvalue. In this regime, stabilisation of $C_2H_5O_2$* is ineffective at all realizable pressures, and the sole products are $C_2H_4 + HO_2$. The smallest eigenvalue now describes reaction (3) and a 'zero pressure' ME model now provides an adequate description of the system, because the reaction occurs so quickly that collisions are ineffective at realizable pressures. Miller and Klippenstein[25] defined a 'stabilization' limit in this context. In this limit, stabilization of $C_2H_5O_2$* is ineffective, 'no matter how high one may make the pressure'.

As discussed above, channels involving reaction (4) and its subsequent dissociation are comparatively ineffective in the ethane system, because they involve transition states which are too high in energy to play a significant role. Formation of QOOH has been implicated in the extensive observations of Walker and co-workers[3] and, as discussed above, this reaction is key to the formation of a range of oxygenated species (aldehydes and cyclic ethers) and is central to degenerate branching.

Very facile formation of OH *via* this route has been observed, even at room temperature, in reactions of oxygenated radicals. CH_3CO reacts with O_2 to form the acetyl peroxy radical, which is an important intermediate in tropospheric chemistry. At low pressures, though, Blitz *et al.*[27] observed formation of OH, which, following earlier, less direct experiments, they ascribed to a mechanism involving reaction (4), to form $CH_2C(O)OOH$, which then dissociates to form OH and the lactone $cCH_2C(O)O$. The transition states for both reaction (4) and the subsequent dissociation lie below the energy of $CH_3CO + O_2$.

The ethyne-OH adduct formed in reaction (1a) (section 5.1) reacts with O_2 in the troposphere, but kinetic measurements demonstrated that the peroxy radical initially formed reacts rapidly to form (i) glyoxal + OH and (ii) formic acid + HCO.[28] The proposed mechanism has been confirmed by *ab initio* calculations[29] showing that the peroxy radical, $HOC_2H_2O_2$, isomerises rapidly *via* an H transfer reaction from the OH group to the peroxy group in channel (i) or forms a cyclic species with the O_2 bridging across the double bond in channel (ii). Both of these species dissociate rapidly, before collisional stabilisation can occur under atmospheric conditions.

Taatjes[24] discussed possible approaches to the direct detection of QOOH. He suggests that low temperature experiments, *e.g.* in supersonic expansions, may be necessary with detection *via* photoionisation mass spectrometry. A key target is its reaction with O_2 and the steps leading to branching. These will undoubtedly be difficult to observe by direct methods. Theory will play a central role in understanding the reaction mechanisms and in helping to design experiments.

There is again an analogy in atmospheric chemistry. Toluene reacts with OH mainly *via* addition to the ring. The

 This journal is © The Royal Society of Chemistry 2008

adduct reacts with O_2 to form a peroxy radical, but formation of the hydroperoxyl radical does not seem to be significant. Instead, the O_2 bridges across the ring and this bicyclic compound goes on to react with another molecule of O_2. Subsequent reactions lead to ring opening and formation of dicarbonyl compounds such as glyoxal. There is also some evidence that OH may be formed.[30] Elucidating this chemistry again presents challenges to both experiment and theory.[29,31,32]

5.2.2 H + SO_2: unravelling the significance of reaction eigenvalues. In this section, we examine the relationship between eigenvalues and phenomenological rate constants for a system with two wells.

The H + SO_2 reaction is important in flames seeded with sulfur and it provides a route to H atom recombination in high temperature flow reactors, *via* H + HOSO → H_2 + SO_2; it is also significant in the general understanding of the role of sulfur in combustion chemistry.[33] The reaction of H atoms with SO_2 proceeds *via* a multi step mechanism, involving the isomer adducts, HSO_2 and HOSO:

$$H + SO_2 \rightleftharpoons HSO_2 \quad (1)$$

$$H + SO_2 \rightleftharpoons HOSO \quad (2)$$

$$H + SO_2 \rightarrow OH + SO \quad (3)$$

$$HSO_2 \rightleftharpoons HOSO \quad (4)$$

$$HSO_2 \rightarrow OH + SO \quad (5)$$

$$HOSO \rightarrow OH + SO \quad (6)$$

Fig. 7 shows a schematic representation of the energies of the stable species and the transition states on the potential energy surface for this reaction. The barriers to reaction are all positive and increase in the order TS1 < TS2 < TS4 < threshold energy for OH + SO, where the transition state numbers refer to the reaction numbers. In addition, the isomer HOSO has a lower zero point energy than HSO_2, which in turn is less than that of H + SO_2.

Blitz *et al.*[33] examined this reaction both experimentally and through ME modelling. There are three chemical species involved in the reaction, H, HSO_2 and HOSO. SO_2 is present in excess and its concentration is incorporated in the pseudo first order rate constant for association, $k'_1 = k_1[SO_2]$. The products, OH and SO, are treated as a sink and the reverse reaction from the products to the HOSO system is not included. The concentration vector of the ME, **c**, is made up of the energy grain concentrations of H, HSO_2 and HOSO, with the concentration of H being represented as a single element in the vector **c**.

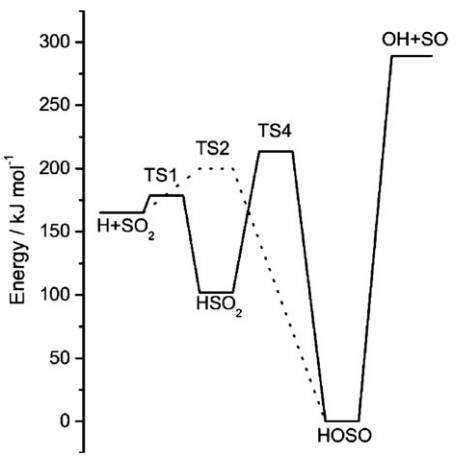

Fig. 7 Potential energy surface for H + SO_2.[29]

At low temperatures the collision matrix for this system has three eigenvalues that differ from the others by several orders of magnitude. These are the chemically significant eigenvalues[11] (CSE—see section 4), and, since there are three species included in **c**, they are associated directly with their reactions and with the phenomenological rate coefficients for the system, $k_1 - k_6$.

Blitz *et al.*[33] analysed the three chemically significant eigenvectors and eigenvalues to relate them to the rate coefficients for each of the reaction steps in the chemical system. The rate equations take the form:

$$\frac{d[HSO_2]}{dt} = k_1[H][SO_2] - k_{-1}[HSO_2] - k_4[HSO_2] + k_{-4}[HOSO] - k_5[HSO_2]$$

with similar differential equations for HOSO and H, based on the chemical mechanism described by reactions (1)–(6). These rate equations can be expressed in matrix form:

$$\frac{d\mathbf{x}}{dt} = \mathbf{K}_C\mathbf{x}$$

where **x** is a vector of the mole fractions of H, HSO_2 and HOSO

$$\mathbf{x} = \begin{pmatrix} [HSO_2] \\ [HOSO] \\ [H] \end{pmatrix}$$

and $\mathbf{K}_C$ is a matrix of rate constants connecting the reactants and products

$$\mathbf{K}_C = \begin{pmatrix} -k_{-1} - k_4 - k_5 & k_{-4} & k_1 \\ k_4 & -k_{-4} - k_{-2} - k_6 & k_2 \\ k_{-1} & k_{-2} & -k_1 - k_2 - k_3 \end{pmatrix}$$

The eigenvalues for this matrix equation correspond to the chemically significant eigenvalues of the master equation, discussed in section 4. Explicit expressions relating the CSE to the phenomenological rate coefficients can be obtained by the diagonalization of $\mathbf{K}_C$. Since there are three eigenvalues, this gives complex algebraic expressions for the CSE, but Blitz *et al.*[33] demonstrated that simpler solutions could be obtained in the limits of high and low temperatures, where $\mathbf{K}_C$ could be approximated to two different 2 × 2 matrices. These could be simplified still further by recognising the dominant rate coefficients, or combinations of rate coefficients, in each eigenvalue expression. Fig. 8 shows, as an example, the results of this analysis for λ_1.

It can be shown that, to a good approximation,[33]

$$|\lambda_1| \approx \frac{k_3[SO_2] + k_6K_2[SO_2]}{1 + K_2[SO_2]}$$

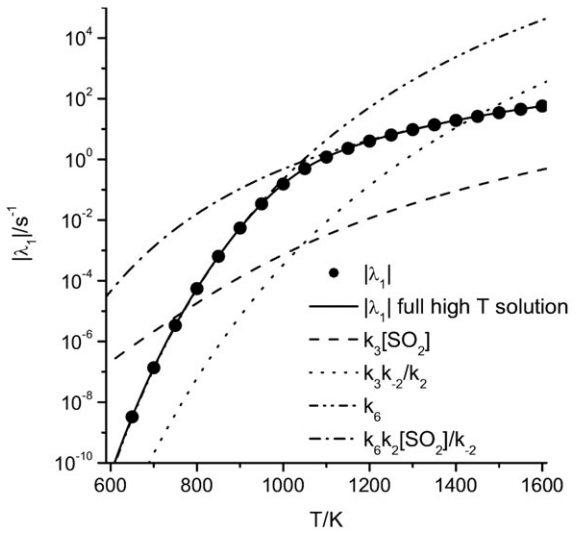

Fig. 8 Relationships between $|\lambda_1|$ for the H + SO_2 reaction system and combinations of rate coefficients, as a function of temperature at 1 atm.[29]

where K_2 is the equilibrium constant for reaction (2). At 1 atm, the term in k_6 is unimportant. At low temperatures, $K_2[SO_2] \gg 1$, so that $|\lambda_1| \approx k_3/K_2 = k_3k_{-2}/k_2$. At high temperatures, $K_2[SO_2] \ll 1$ and $|\lambda_1| \approx k_3[SO_2]$ (see Fig. 8): the eigenvalue is determined by reaction (3), formation of OH + SO from H + SO_2. The term in K_2 reflects the requirement, at low temperatures, to correct the concentration of H for the fraction tied up as HSO_2; at higher temperatures, the position of equilibrium lies with the reactants (H + SO_2), so that the correction becomes unnecessary. Fig. 8 shows that reaction (6) makes a negligible contribution to $|\lambda_1|$ and formation of OH + SO occurs predominantly from H + SO_2 *via* the energised states of HOSO—an indirect reaction. Blitz *et al.*[33] showed that reaction (6), involving stabilised HOSO, only becomes significant at much higher pressures: it is the dominant route at 10^6 atm.

Blitz *et al.*[33] showed that each eigenvalue could be associated with passage over a single energy barrier, in agreement with observations made earlier by of Miller and Klippenstein.[16] λ_3 is associated with TS1, λ_2 with TS2 and λ_1 with the transition state separating HOSO and OH + SO. Reactions (R4) and (R5) were not significant, because reaction of HSO_2 to form H + SO_2 is always much faster than that to form HOSO, so that TS4 plays no significant role in the reaction.

k_2 and k_3 increase with pressure to an asymptote, showing a similar behaviour to that shown in Fig. 1 and 2. k_4, on the other hand, *decreases* from a *low* pressure asymptote as the pressure increases, because collisional stabilisation to form HOSO depletes the energised states of HOSO directly populated from H + SO_2, thus decreasing the rate of the indirect reaction forming OH + SO from H + SO_2. More complex pressure dependences were obtained for k_4 and k_6, whose forms are not fully understood.

6. Evaluations of kinetic data

There are inherent uncertainties in kinetic measurements. Some are statistical and derive from random errors associated, for example, with noise in the signal. Other sources are systematic, deriving, for example, from secondary reactions that affect the signal whose form is then not solely due to the single reaction under study. More accurate measurements can be made by increasing the sensitivity of the detection technique, so that it is possible to work at lower reactant radical concentrations and hence reduce the impact of secondary reactions. It is also possible to build a model of the competing reactions, and make allowances for them in deriving the rate coefficient for the reaction under study. Even so, there are often significant discrepancies between rate coefficients derived using different methods and/or from different laboratories. This problem has led to the establishment of groups of experts who *evaluate* the available rate data.[34] The group examines the methods that have been used to measure specific reactions, and, on the basis of the data and their assessment of the experimental methods, they make a reasoned recommendation of the rate coefficient expression over a specific range of temperature and, if appropriate, pressure. They also recommend an uncertainty range for the rate coefficient parameters. The resulting tabulations provide an essential resource for modellers and those constructing chemical mechanisms. The assessments also provide a means of identifying reactions in need of further study. As yet, evaluation panels make little use of theoretical determinations of rate coefficients. The considerable advances that have been made in theory in recent years make this neglect increasingly untenable.

7. Conclusions

Considerable advances have been made in both experiment and theory. Increasingly complex reactions are investigated experimentally; a particularly important development has been the measurement of absolute channel yields, such as the yield of HO_2 from R + O_2 reactions. *Ab initio* calculations can produce energies for transition states that are beginning to rival the accuracy of experimental values, especially at combustion temperatures. They also provide an unparalleled means of understanding how reactions proceed. Master equation methods can now deal with quite complex reactions and return rate coefficients for individual reaction steps. The next few years are likely to see a substantial exploitation of these developments, largely through an increased interaction between theory and experiment.

Acknowledgements

I am grateful to my colleagues at Leeds, and especially to Mark Blitz, David Glowacki, Kevin Hughes, Struan Robertson and Paul Seakins for their many contributions to our work together on reaction kinetics. EPSRC and NERC are acknowledged for funding.

References

1 J. F. Griffiths and J. A. Barnard, *Flame and Combustion*, Blackie, London, 3rd edn, 1995.
2 C. A. Taatjes, N. Hansen, J. A. Miller, T. A. Cool, J. Wang, P. R. Westmoreland, M. E. Law, T. Kasper and K. Kohse-Hoeinghaus, *J. Phys. Chem. A*, 2006, **110**, 3254.

 This journal is © The Royal Society of Chemistry 2008

3 R. W. Walker and C. Morley, in *Low-Temperature Combustion and Autoignition*, ed. M. J. Pilling, Elsevier, Amsterdam, The Netherlands, 1997, p. 1.
4 S. H. Robertson, P. W. Seakins and M. J. Pilling, in *Low-Temperature Combustion and Autoignition*, ed. M. J. Pilling, Elsevier, Amsterdam, The Netherlands, 1997, p. 125.
5 P. A. Cleary, M. T. B. Romero, M. A. Blitz, D. E. Heard, M. J. Pilling, P. W. Seakins and L. Wang, *Phys. Chem. Chem. Phys.*, 2006, **48**, 5633.
6 E. P. Clifford, J. T. Farrell, J. D. DeSain and C. A. Taatjes, *J. Phys. Chem. A*, 2000, **104**, 11549.
7 H. Qian, D. Turton, P. W. Seakins and M. J. Pilling, *Chem. Phys. Lett.*, 2000, **322**, 57.
8 A. J. Eskola and R. S. Timonen, *Phys. Chem. Chem. Phys.*, 2003, **5**, 2557.
9 S. S. Brown, A. R. Ravishankara and H. Stark, *J. Phys. Chem. A*, 2000, **104**, 7044.
10 N. K. Srinivasan, M.-C. Suz and J. V. Michael, *Phys. Chem. Chem. Phys.*, 2007, **9**, 4155.
11 M. A. Oehlschlaeger, D. F. Davidson and R. K. Hanson, *J. Phys. Chem. A*, 2006, **110**, 9867.
12 K. Kohse-Hoeinghaus, R. S. Barlow, M. Alden and J. Wolfrum, *Proc. Combust. Inst.*, 2004, **30**, 89.
13 L. B. Harding, S. J. Klippenstein and A. W. Jasper, *Phys. Chem. Chem. Phys.*, 2007, **9**, 4055.
14 K. A. Holbrook, M. J. Pilling and S. H. Robertson, *Unimolecular Reactions*, Wiley, London, 1996.
15 S. H. Robertson, M. J. Pilling, L. C. Jitariu and I. H. Hillier, *Phys. Chem. Chem. Phys.*, 2007, **9**, 4085.
16 S. J. Klippenstein and J. A. Miller, *J. Phys. Chem. A*, 2002, **106**, 9267.
17 K. W. McKee, M. A. Blitz, P. A. Cleary, D. R. Glowacki, M. J. Pilling, P. W. Seakins and L. M. Wang, *J. Phys. Chem. A*, 2007, **111**, 4043.
18 J. W. Davies, N. J. B. Green and M. J. Pilling, *Chem. Phys. Lett.*, 1986, **126**, 373.
19 J. Troe, *J. Phys. Chem.*, 1979, **83**, 114.
20 J. P. Senosiain, S. J. Klippenstein and J. A. Miller, *J. Phys. Chem. A*, 2005, **109**, 6045.
21 E. E. Greenwald, S. W. North, Y. Georgievskii and S. J. Klippenstein, *J. Phys. Chem. A*, 2005, **109**, 6031.
22 D. Bradley and C. Morley, in *Low-Temperature Combustion and Autoignition*, ed. M. J. Pilling, Elsevier, Amsterdam, The Netherlands, 1997, p. 661.
23 J. F. Griffiths and C. Mohamed, in *Low-Temperature Combustion and Autoignition*, ed. M. J. Pilling, Elsevier, Amsterdam, The Netherlands, 1997, p. 545.
24 C. A. Taatjes, *J. Phys. Chem. A*, 2006, **110**, 4299.
25 J. A. Miller, S. J. Klippenstein and S. H. Robertson, *Proc. Combust. Inst.*, 2000, **28**, 1479.
26 J. A. Miller and S. J. Klippenstein, *Int. J. Chem. Kinet.*, 2001, **33**, 654.
27 M. A. Blitz, D. E. Heard and M. J. Pilling, *Chem. Phys. Lett.*, 2002, **365**, 374.
28 Z. Y. Zhang and J. Peeters, in *Proceedings Fifth European Symposium on Physico-Chemical Behaviour of Atmospheric Pollutants*, ed. G. Restelli and G. Angeletti, Kluwer Academic Publishers, Dordrecht, 1990, p. 377.
29 D. R. Glowacki, PhD Thesis, University of Leeds, 2007.
30 C. Bloss, V. Wagner, M. E. Jenkin, R. Volkamer, W. J. Bloss, J. D. Lee, D. E. Heard, K. Wirtz, M. Martin-Reviejo, G. Rea, J. C. Wenger and M. J. Pilling, *Atmos. Chem. Phys.*, 2005, **5**, 641.
31 S. Raoult, M.-T. Rayez, J.-C. Rayez and R. Lesclaux, *Phys. Chem. Chem. Phys.*, 2004, **6**, 2245.
32 F. Motta, G. Ghigo and G. Tonachini, *J. Phys. Chem. A*, 2002, **106**, 4411.
33 M. A. Blitz, K. J. Hughes, M. J. Pilling and S. H. Robertson, *J. Phys. Chem. A*, 2006, **110**, 2996.
34 D. L. Baulch, C. T. Bowman, C. J. Cobos, R. A. Cox, T. Just, J. A. Kerr, M. J. Pilling, D. Stocker, J. Troe, W. Tsang, R. W. Walker and J. Warnatz, *J. Phys. Chem. Ref. Data*, 2005, **34**, 757.